communications earth & environment

Article

https://doi.org/10.1038/s43247-024-01301-1

A temporal control on the isotopic compositions of the Antarctic Peninsula arc

Joaquin Bastias-Silva [1,2,5] ✉, Alex Burton-Johnson [3], David Chew[1], Teal Riley[3], Wuidad Jara [2] & Massimo Chiaradia [4]

Radiogenic isotopic compositions of arc magmas are a key tool for studying active margin evolution. They have two isotopic end-members: melts formed mostly from juvenile asthenosphere and melts sourced from evolved continental crust/continental lithospheric mantle. Cordilleran-margins are typically more isotopically juvenile near the trench, and conversely, increasingly evolved landward. However, this model has not been tested on the ~1,500 km long Mesozoic-Cenozoic arc of the Antarctic Peninsula. Here we show that while geochemical compositions remain largely constant, radiogenic isotopes become increasingly juvenile with time. Unlike other continental arcs, there is no association between isotopic composition and spatial distribution. This is attributed to: (i) slow subduction of young oceanic lithosphere, resulting in narrowing of the arc and reduced capacity to incorporate continental crust into melts, and (ii) the Cenozoic decrease in convergence rate, which reduced the friction in the slab-overriding plate interface, allowing the arc melts to increasingly source from young juvenile asthenosphere.

Spatial and temporal changes in the radiogenic isotopic composition of arc magmatism is a fundamental tool for studying the interactions between the crust and the lithosphere in convergent margins[1,2]. These changes have been used to interpret diverse tectonic phenomena including continental subduction[3], slab-dip[4], subduction rate[5], subduction erosion[6], delamination[7], changes in crustal thickness[8], and lithospheric extension[9] among others. Spatial trends in the radiogenic isotopic composition of arc magmatism have been interpreted as an intrinsic feature of Cordilleran-style orogenic systems[2] and likely imply a fundamental change in the dynamics governing the formation of their igneous rocks. A consistent trend has been observed in arc magmas from the Central Andes, U.S. Cordillera and Tibet, whereby more isotopically juvenile compositions are encountered near the trench (i.e. radiogenic or enriched $^{176}Hf/^{177}Hf$ and $^{143}Nd/^{144}Nd$) and increasingly evolved trench-distal (unradiogenic or depleted $^{176}Hf/^{177}Hf$ and $^{143}Nd/^{144}Nd$[2]). Furthermore, these Cordilleran systems are well-studied examples of both modern and ancient active margins, which suggest that this spatial-compositional trend is long-lived and persists throughout the life of a given continental arc. Additionally, these spatial trends are observed in a broad spectrum of geochemical compositions. These spatial isotopic trends for Cordilleran magmatism have been explained by the mantle lithosphere thinning towards the trench due to sub-lithospheric processes, such as delamination or subduction erosion, allowing the magmas to be sourced from isotopically juvenile asthenospheric mantle with minimal lithospheric interaction[2]. Conversely, isotopically evolved arc magmas are founded landward, where the absence of lithospheric thinning permits the development of a thicker continental mantle lithosphere, producing isotopically evolved arc magmas.

The Antarctic Peninsula represents the southern terminus of America's cordilleran arc (i.e. western border of Northern, Central and South America), which is arguably continuous from the western Aleutians[10] to the Antarctic Peninsula[11], with the exception of the San Andreas fault[12] in North America. Although difficult access has partially hindered its understanding and characterisation, a plethora of recent data now permits a more robust characterisation of this Mesozoic-Cenozoic continental margin[13–22]. The Antarctic Peninsula thus makes an excellent natural laboratory for both testing and revising the dynamics in Cordilleran convergent margins. We combine these existing datasets with newly presented geochemistry (elemental and isotopic) and geochronology from the Cenozoic arc record,

[1]Department of Geology, Trinity College Dublin, College Green, Dublin 2, Dublin, Ireland. [2]Escuela de Geología, Facultad de Ingeniería, Universidad Santo Tomás, Santiago, Chile. [3]British Antarctic Survey, High Cross, Madingley Road, Cambridge, CB3 0ET Cambridge, UK. [4]Department of Earth Sciences, University of Geneva, Geneva, 1205 Geneva, Switzerland. [5]Present address: Institute of Geochemistry and Petrology, Department of Earth Sciences, ETH Zürich, Zürich, Switzerland. ✉e-mail: j.bastias.silva@gmail.com

providing key information for a poorly constrained period of the Antarctic Peninsula. We use these combined datasets to test the model proposed for other Cordilleran-active margins and examine the magmatic and tectonic history of the Antarctic Peninsula in comparison with the Central Andes, U.S. Cordillera and Tibet[2]. These are long-lived and well-studied convergent margins, which have been fundamental to build the knowledge we have on the evolution of arc magmatism[2,23–26].

Results and discussion

The active margin of the Antarctic Peninsula: a Mesozoic-Cenozoic history

The Antarctic Peninsula orogenic system developed above the eastward-subducting oceanic lithosphere of the Phoenix Plate and represents one of the major magmatic arcs of the circum-Pacific rim extending for almost 1500 km south from the Drake Passage (Fig. 1). This convergent margin developed as an autochthonous continental arc on the margin of Gondwana[11,14,27–29]. It is considered to have initiated as early as the Triassic[14,17,30] and the subduction system waned during the Cenozoic[20,22,31,32]. Cessation of subduction progressively occurred from south to north during the Cenozoic as a consequence of ridge-trench collisions of the Antarctic-Phoenix Plate system with the west margin of the Antarctic Peninsula[32]. Subduction finally ceased concurrently with the end of Antarctic-Phoenix spreading at ~3 Ma[33]. Continuing sinistral relative motion of South America and Antarctica was accommodated by transtensional opening of the Bransfield Strait as a pull-apart basin[34,35]. Under this regional transtensional regime without active subduction, low-volume alkaline magmatism commenced at ~15 Ma and is ongoing[36,37].

Geochemistry: nearly changeless

The whole rock major and trace element compositions of the convergent margin magmatism of the Antarctic Peninsula exhibit little variation for different time windows during the Mesozoic and Cenozoic (Fig. 2), with the exception of a shift from being peraluminous-dominant during the Triassic-Jurassic to metaluminous-dominant during the Cretaceous-Cenozoic (Fig. 2a). Nevertheless, they consistently show a strong affinity to volcanic arc granite compositions (Fig. 2b). Strong similarities are also observed in N-MORB normalised trace element abundances, showing in general an enrichment in Light Ion Lithophile Elements (LILE) and negative Nb, Ta and Ti anomalies, suggesting a subduction-derived component in their source. They also exhibit minor negative Eu anomalies, which suggests that plagioclase has fractionated, and the positive Pb anomaly is likely to have been derived from an upper crustal source[38] (Fig. 2c). A lack of temporal trends in the La_n/Yb_n and Sr/Y plots (Fig. 2d) throughout the Mesozoic-Cenozoic suggest that the crustal thickness of the arc did not change during this period[39,40]. However, estimates of continental arc crustal thickness using geochemical indices are problematic due to the multiple petrogenetic processes that occur in this setting[41], and these should perhaps only be used as qualitative indicators[42].

Isotopic compositions: time sensitive

In situ Lu-Hf isotopic compositions from zircon were compiled and complemented with Sm-Nd and Rb-Sr whole-rock isotopic data from the active margin igneous rocks of the Antarctic Peninsula (Fig. 3). Analysis of inherited zircon cores yield abundant Palaeozoic ages, which have been interpreted as having formed on the active margin of southwestern Gondwana[14] and thus autochthonous to the Antarctic Peninsula. Furthermore, zircons formed during the Ordovician-Triassic yield Hf-isotopic compositions that broadly follow the evolution of the average bulk crustal source[43] (Fig. 3a). This suggests that during the Palaeozoic there was not a relevant amount of primordial isotopically juvenile sources incorporated in these old arc magmas. During the Jurassic-Cretaceous, zircons yield Hf-isotopic compositions that suggest mixing between juvenile and evolved crustal sources. Isotopically juvenile compositions are dominant during the Palaeogene, which imply greater influence of the asthenospheric mantle in the sources of arc magmatism during this time period. Sm-Nd and Rb-Sr whole-rock isotopic compositions from igneous rocks broadly follow the Hf isotope in zircon trends observed for the Mesozoic-Cenozoic (Fig. 3b). They show a transition from the Triassic to the Cenozoic rocks, whereby they evolve from more isotopically evolved to juvenile magmas.

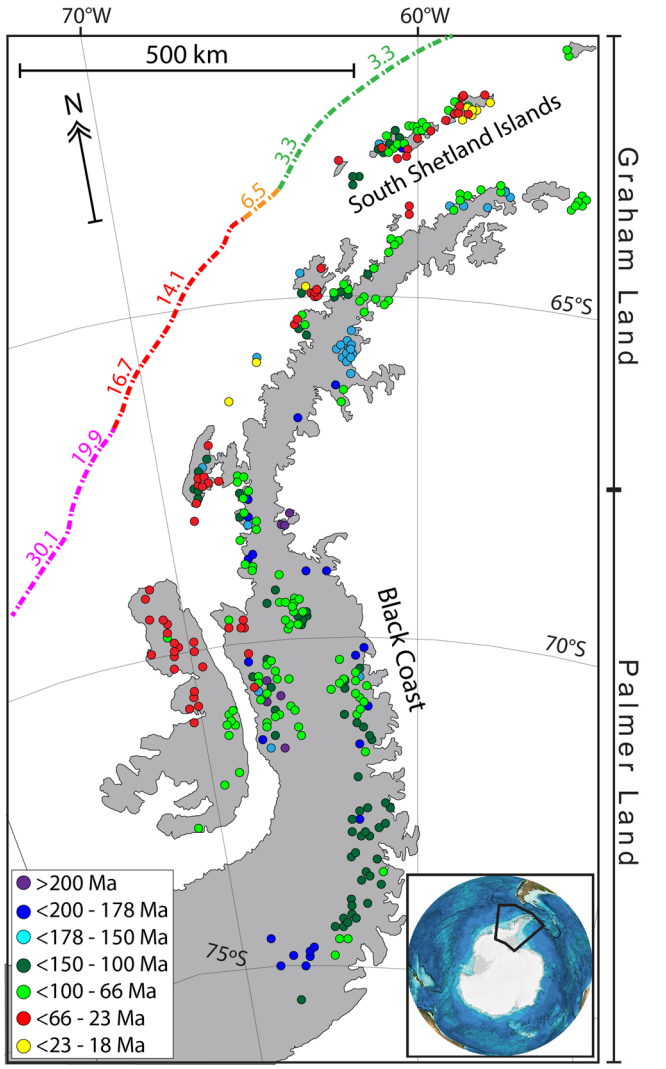

Fig. 1 | Arc magmatic ages in the Antarctic Peninsula. Magmatic age compilation used in this work (Supplementary Material: https://doi.org/10.5281/zenodo.10605934) along with estimated ages for subduction cessation by refs. 46,84. The inserted map showing Antarctica and Patagonia was generated by Google Earth™.

The complex spatial relationship

The spatial distribution of igneous rocks with time is a fundamental tool for understanding the evolution of subduction-related magmatism[2,22]. We have used the geographic position of the igneous arc rocks and calculated the shortest distance to the trench. Although subduction is presently inactive, the trench remains observable as a prominent bathymetric depression along the western margin of the Antarctic Peninsula. The distance of a given arc pluton with respect to the continent-ocean boundary (COB) is plotted in Fig. 4a (locus of arc magmatism with time) and shows that (i) the position of the most proximal arc magmatism relative to the trench has remained broadly static with time, maintaining a consistent distance of ~100–150 km, and (ii) from ~100 Ma onwards the most distal arc magmas progressively migrate to the trench at ~6 km/Myr[22] (Fig. 4a). This migration and resultant arc-narrowing results primarily from the arrival of progressively younger oceanic lithosphere at the trench with each ridge-trench collision. Because of the broadly north-south orientation of the Antarctic Peninsula, latitude is a convenient parameter to analyse spatial trends with time along the arc

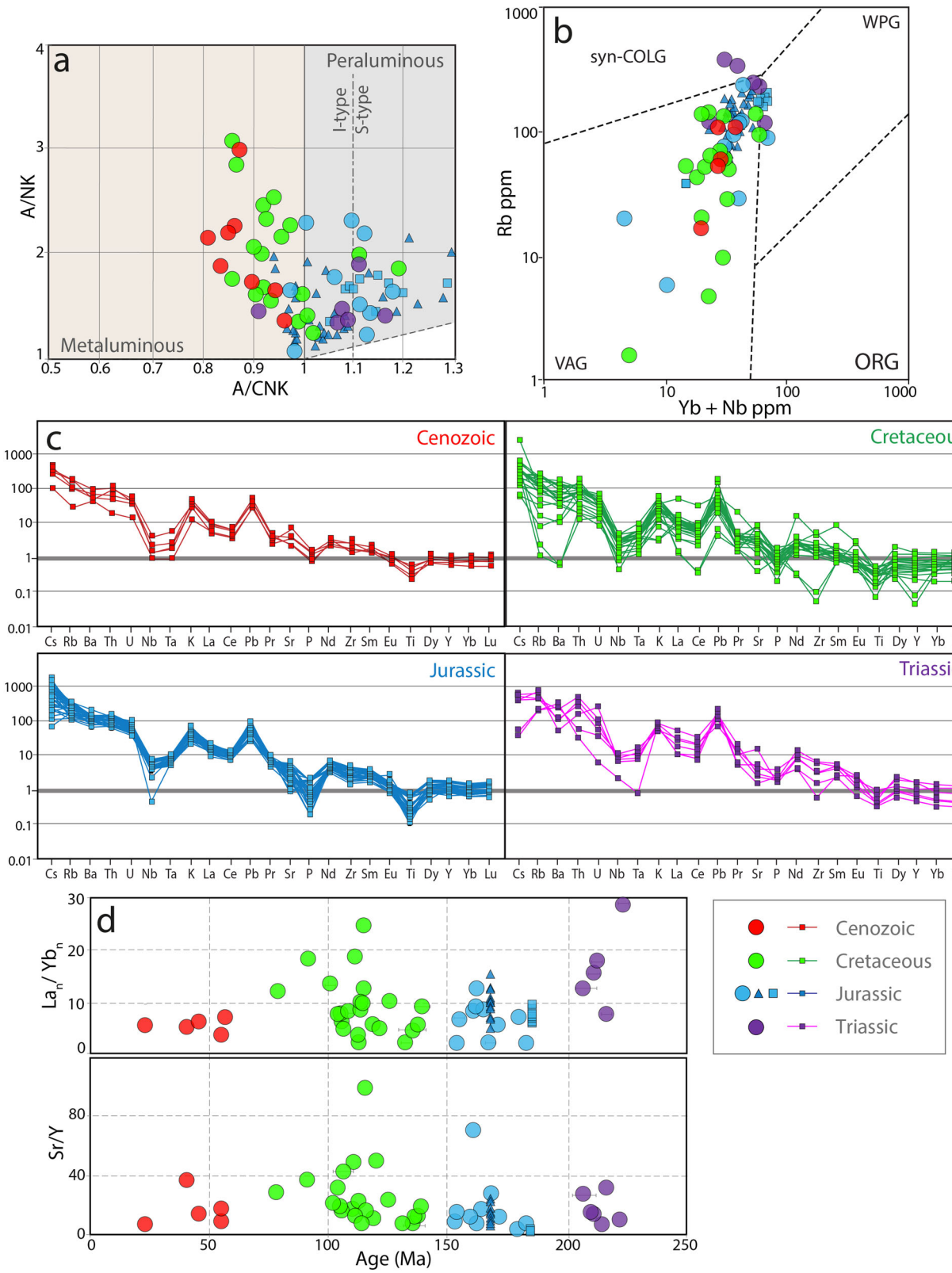

Fig. 2 | Geochemical compilation of the arc magmas of the Antarctic Peninsula. **a** Aluminium saturation index (ASI) plot[85], (Al/Na+K) and (Al/Ca+Na+K) are defined as molecular ratios and take into account the presence of apatite so that rocks with ASI N 1.0 are corundum normative and are termed peraluminous[86]. **b** Rb vs Yb + Nb discrimination diagram for tectonic settings from[87]. WPG within plate granites, VAG volcanic arc granites, ORG ocean ridge granites, syn-COLG syn-collisional granites. **c** Rare earth element and trace element abundances normalised to the N-MORB values of ref. 88. **d** Diagrams showing La_n/Yb_n and Sr/Y versus age. The full dataset is included in the Supplementary Material (https://doi.org/10.5281/zenodo.10605934).

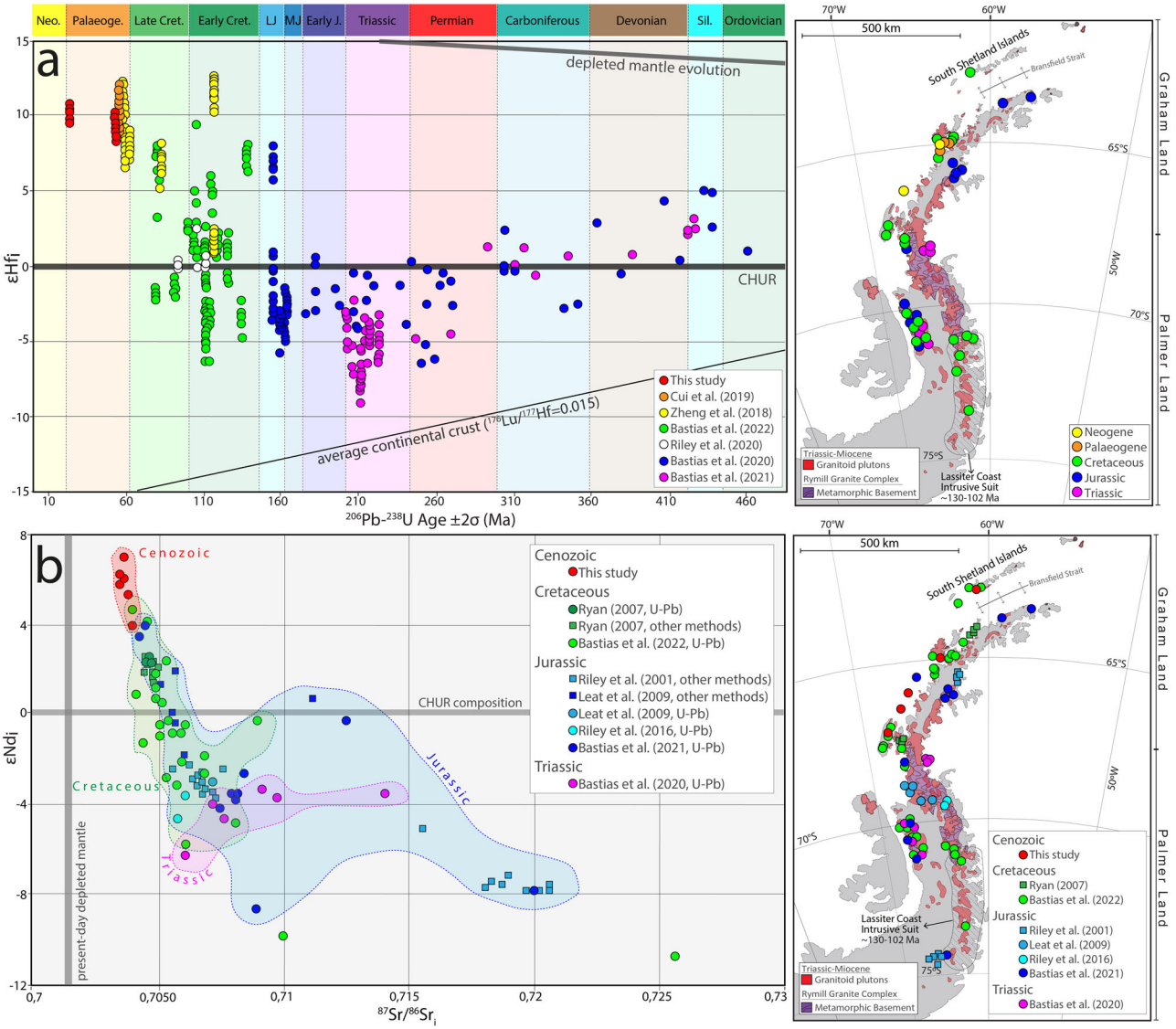

Fig. 3 | Isotopic tracing compilation of the arc magmas of the Antarctic Peninsula. a Comparison of the ^{206}Pb-^{238}U zircon ages and zircon εHf_i for crystals from the igneous rocks of the active margin of the Antarctic Peninsula. The 2σ uncertainties are ~±5% for U–Pb zircon ages. **b** Comparison of the εNd_i and $^{87}Sr/^{86}Sr_i$ values of the igneous rocks of the active margin of the Antarctic Peninsula. Sources are colour-coded. $^{176}Lu/^{177}Hf = 0.015$ for the average continental crust[43]. The full dataset is included in the Supplementary Material (https://doi.org/10.5281/zenodo.10605934).

margin (Fig. 4b). This reveals that arc magmatism ceased at ~20–19 Ma along a relevant segment of the margin, from ~67–62°S, and shows the progressive northward cessation from ~100 Ma. Nd isotopic compositions of the arc magmatic rocks of the Antarctic Peninsula do not show a clear relationship with their distance from the trench (Fig. 4c), with both juvenile compositions (i.e. $\varepsilon Nd_i > 5$) and evolved compositions ($\varepsilon Nd_i < 0$) located from ~200 km up to ~450 km from the trench. This argues against a strong correlation between radiogenic isotopic compositions and distance to the trench observed in other Cordilleran orogens[2]. Nevertheless, the Nd-isotopic compositions of these rocks show a strong correlation with their crystallisation age (Fig. 4d), with a tendency towards more isotopically juvenile compositions with younger ages from ~100 Ma onwards. Juvenile Nd-isotopic compositions become dominant in the Cenozoic, which agrees well with the Hf-isotopic compositions in zircon data (Fig. 3a) and implies coupled behaviour between these two isotopic systems.

The evolution of the Antarctic Peninsula active margin

From our compilation of geochronological, geochemical and isotopic data, the arc magmatic rocks that formed during the Mesozoic and early Cenozoic along the convergent margin of the Antarctic Peninsula exhibit a wide range in distances to the trench and in their radiogenic isotopic compositions (Figs. 3, 4). During the Mesozoic, relatively diverse magma compositions and variable degrees of crustal assimilation are encountered, coincide with the subduction of the relatively old (i.e. >~40 Myr) oceanic lithosphere of the Phoenix Plate beneath the continental lithosphere of the Antarctic Plate[22,44] (Fig. 5a).

During the Late Cretaceous and Palaeogene, the progressively younger oceanic lithosphere of the Phoenix Plate was subducted beneath the Antarctic Peninsula[22,32] (Fig. 5b). This process is marked by: (i) progressive migration of magmatism at the rear of the arc towards the trench (Fig. 4a) resulting in the narrowing of the belt of arc magmatism; (ii) progressively more juvenile radiogenic isotopic compositions (Figs. 3, 4); and (iii) the northward-progressive collision of ridge-trench segments, causing the wane and eventual cessation of subduction. Our new data indicates that the last magmatic products of the arc date to ~20–19 Ma, which confirms previous studies[31,45] along with recent findings[22]. This not only represents the last phase of arc magmatism in the Antarctic Peninsula, but also the Antarctic continent as a whole. Furthermore, they[22] numerically related the slab age, convergence rate and slab dip of the Antarctic-Phoenix system to show that the narrowing of the arc and the cessation of arc magmatism in the Antarctic

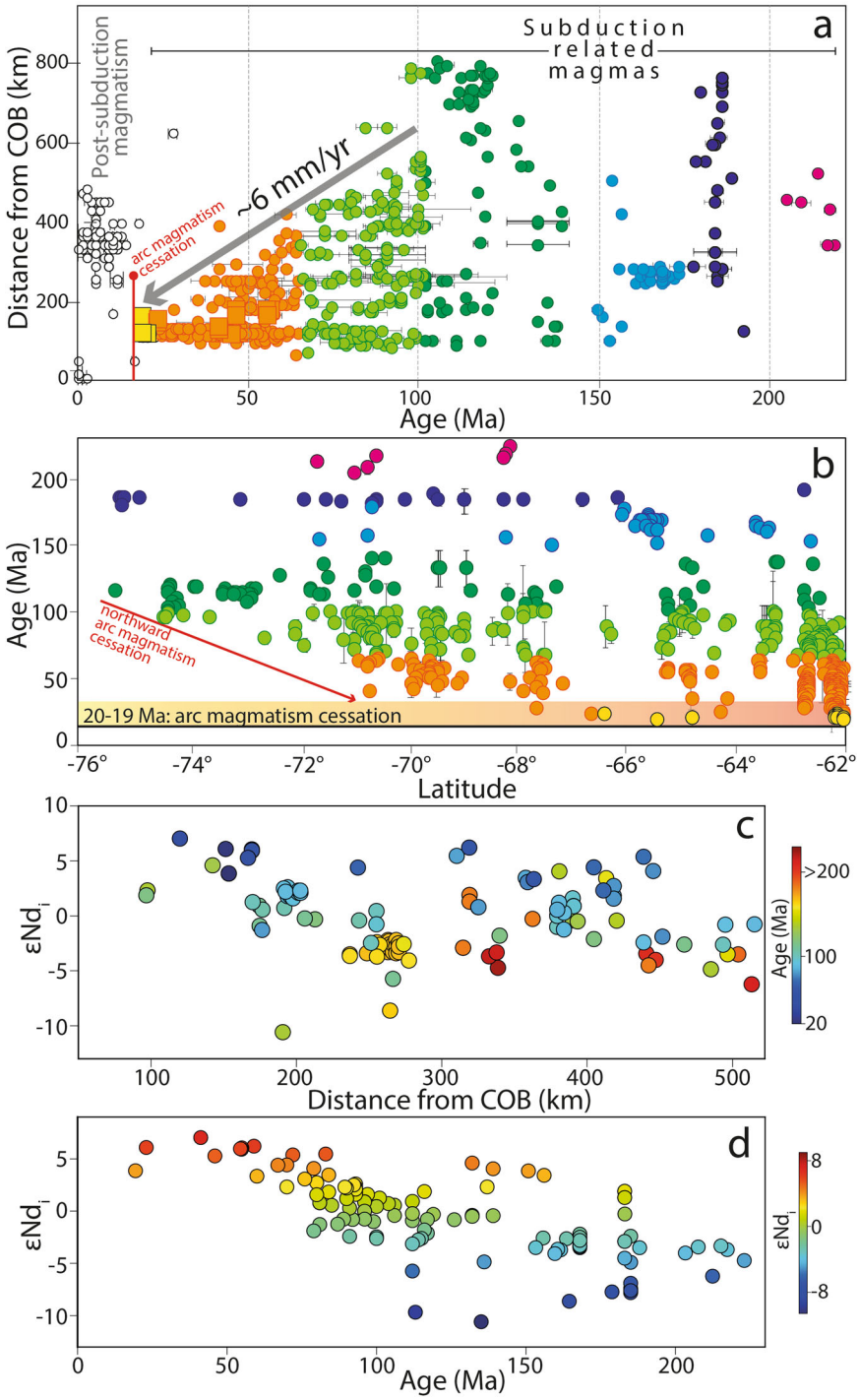

Fig. 4 | Comparison of distance from the continent-ocean boundary (COB), crystallisation age, latitude, and εNd_i of the igneous rocks of the active margin of the Antarctic Peninsula. **a** Comparison of distance from the COB and crystallisation age, adapted from[22]. **b** Comparison of crystallisation age and latitude. **c** Comparison of distance from the COB and εNd_i, with crystallisation age denoted by a colour ramp. **d** Comparison of crystallisation age and εNd_i. Full dataset is presented in the Supplementary Material (https://doi.org/10.5281/zenodo.10605934).

Peninsula was primarily in response to the subduction of progressively younger oceanic lithosphere along with a slower convergence rate. This suggests that slab age and convergence rate may affect the magmatic arc geometry and compositions in settings that are commonly attributed to slab-dip variation.

While successive ridge-trench collisions of the Antarctic-Phoenix system with the western margin of the Antarctic Peninsula caused the waning and cessation of arc magmatism (culminating at ~20–19 Ma), these collisions effectively occurred ~8–5 Myr after arc magmatism had ceased[22] (Fig. 5c). The occurrence of amagmatic subduction for ~8-5 Myr after final arc magmatic cessation at ~20-19 Ma implies subduction effectively ceased by ~15-12 Ma across most of the northern Antarctic Peninsula. Subduction continued in three segments of the Phoenix Plate, located to the north of the Hero Fracture Zone (Fig. 5c) albeit at a much slower rate until ~3 Ma[32,33,46]. Nevertheless, arc magmatism also waned at ~20-19 Ma in this sector[31], as it had along the rest of the Antarctic Peninsula margin.

Comparison with other Cordilleran-style subduction systems. Compilations of Lu-Hf, Sm-Nd, Rb-Sr and Pb isotopic data on magmatic rocks have been used as a tool to understand how active margin orogens evolve with time[2,15,16,23,24,26,47,48]. We present a compilation of Lu-Hf and Sm-Nd isotopic compositions of magmatic rocks from three long-lived convergent margins[2]: (i) the Central Andes, an active cordilleran margin; (ii) the western United States (U.S.) Cordillera, an ancient active margin; and (iii) Tibet, an active margin that has transitioned into a continental collisional orogen following India-Asia collision. These other Cordilleran

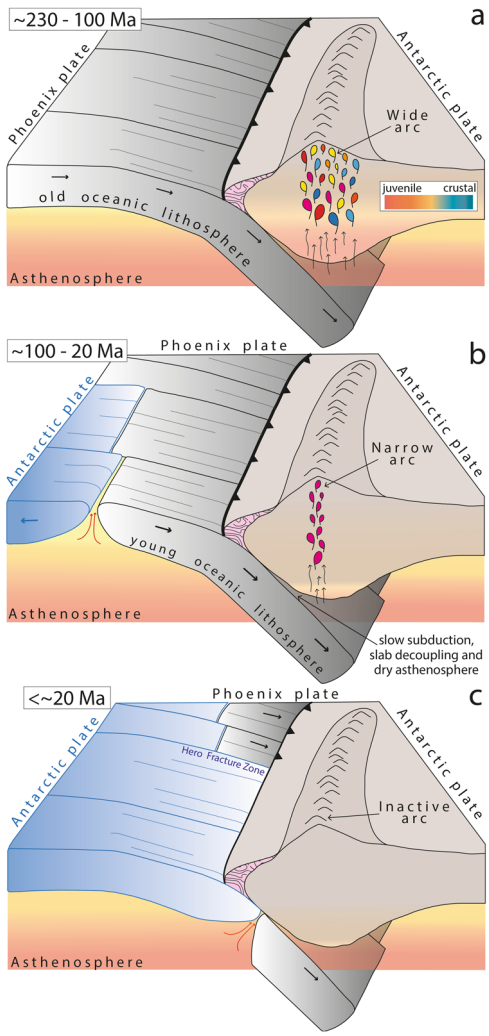

Fig. 5 | Schematic diagrams showing the sequential evolution of the active margin of the Antarctic Peninsula. a Prior to ~100 Ma, the subduction system was dominated by the subduction of the old oceanic lithosphere of the Phoenix Plate, developing a wide arc with juvenile to evolved radiogenic isotopic compositions. **b** From ~100 to ~20 Ma, subduction of the progressively younger Phoenix Plate oceanic lithosphere produced a narrower arc with progressively more juvenile radiogenic isotopic compositions. **c** Post ~20 Ma, subduction ceased along most of the margin following the ridge-trench collision of the Antarctic-Phoenix system.

orogens have a distinctive spatial-temporal pattern in the radiogenic isotopic compositions of their igneous rocks, displaying more isotopically juvenile compositions near the (paleo-) trench and increasingly evolved isotopic compositions landward (Fig. 6). This suggests that the isotopic composition of magmatism at any given location in the orogenic system varies within a limited isotopic range throughout the life of the continental arc[2], and thus contemporaneous magmatism has different isotopic compositions when emplaced at variable distances from the trench. Furthermore, these magmas exhibit a range of geochemical compositions, suggesting that this spatial trend may be an inherent feature of active margin systems.

The Tibetan, Central Andes, and U.S. Cordillera yield a strong correlation between the distance to the trench and their isotopic compositions (Fig. 6a,b,c). The distance to the trench in the Tibetan orogen system is measured with respect to the Indus-Yarlung suture (Fig. 6a), along which oceanic lithosphere was subducting northward beneath Asia prior to the subduction of the Indian plate[25]. The distance to the trench in the U.S. Cordillera is measured by the longitude, which is a useful trench-distance parameter given the approximate east-directed subduction direction of the oceanic lithosphere (Farallon Plate) (Fig. 6b). Similarly, the Central Andes also have east-directed subduction whereby the Nazca Plate oceanic lithosphere subducts under the South American continental lithosphere, and thus longitude is again the chosen trench-distance parameter (Fig. 6c). The colour ramps presented in Fig. 6 show the distribution of the magmatic ages, allowing comparison of their crystallisation age, isotopic composition, and distance to the trench. As it has been shown[2], the correlation between the isotopic compositions of the magmas and their distance to the trench is independent of age (Fig. 6a, b, c). However, the arc magmatic rocks from the Antarctic Peninsula do not exhibit this spatial-isotopic trend (Fig. 6d), yielding isotopically juvenile compositions with a wide range of distances from the trench, as do the more isotopically evolved compositions. As shown previously, the igneous rocks of the active margin of the Antarctic Peninsula exhibit a much stronger correlation with their crystallisation age (Figs. 3, 4d).

Implications for active margin dynamics. Melts extracted from the convecting asthenospheric mantle are (continually) depleted in Hf/Lu and Nd/Sm[49] and exhibit isotopically juvenile compositions. Conversely, in an isotopically closed system, magmas assimilating older continental crust will be more isotopically evolved than those magmatic products that assimilate more juvenile continental crust. This principle renders radiogenic isotopic systems a powerful tool to understand the evolution of active margin dynamics. Evolved or juvenile isotopic compositions may not be necessarily related to the degree of magmatic differentiation (i.e. the change from mafic to felsic bulk compositions) and thus, bulk geochemistry may be decoupled from the isotopic compositions of a given rock[50]. This is one of the main advantages of using radiogenic isotopic tracing over bulk rock compositions for assessing mantle-crust dynamics in active margins. If there is crustal assimilation throughout the evolution of a given magmatic system, bulk rock compositions can potentially be linked to the isotopic evolution[50]. However, the arc magmatic rocks from the Antarctic Peninsula show relatively constant geochemical compositions throughout the life of the margin (Fig. 2), but radiogenic isotopes exhibit a clear shift at ~100 Ma in both the Lu-Hf and the Sm-Nd systems (Figs. 3, 4d).

The spatial relationship between the distance to the trench with the isotopic compositions observed in other active margins[2] is not clearly observed in the Antarctic Peninsula (Fig. 6) and therefore, the causative mechanisms for this trend proposed for other active margins may not be applicable to the Antarctic Peninsula. The relationship between the isotopic compositions with distance to the trench in Cordilleran margins has been primarily explained by the relative presence or absence of continental mantle lithosphere[2] (which produces evolved or juvenile compositions, respectively). In contrast, the Antarctic Peninsula shows a progressive evolution towards more juvenile compositions (Figs. 3,4d) and a narrowing of the arc (Fig. 4a) from the Late Cretaceous onwards. Furthermore, it is possible to observe a progressive narrowing of the arc, with the arc front maintaining a distance of ~150–100 km and the rear of the arc migrating towards the trench (Fig. 4a). The waning of Phoenix Plate subduction beneath the Antarctic Peninsula has been associated with roll-back[45] and slab window processes[51]. However, recently this process has been modelled[22] and showed that the narrowing of the Antarctic Peninsula arc primarily results from the subduction of progressively younger oceanic lithosphere and secondarily with a decrease in convergence rate. This argues against the formation of isotopically juvenile magmas by a slab roll-back mechanism, as in that case the front of the arc should migrate trenchward but instead the arc front maintains a steady position relative to the trench (Fig. 4a). A slab window mechanism is not supported either, because arc magmatism ceased ~5–8 Myr prior to the ridge-trench collisions and thus the slab window event postdates the youngest subduction magmas[27]. However, we acknowledge that a slab window may have developed after the ridge-trench collisions of the Antarctic-Phoenix system, as it has been suggested[51].

We suggest that the progressive narrowing of the arc by the migration of its rear from ~100 Ma onwards played a pivotal role in the generation of

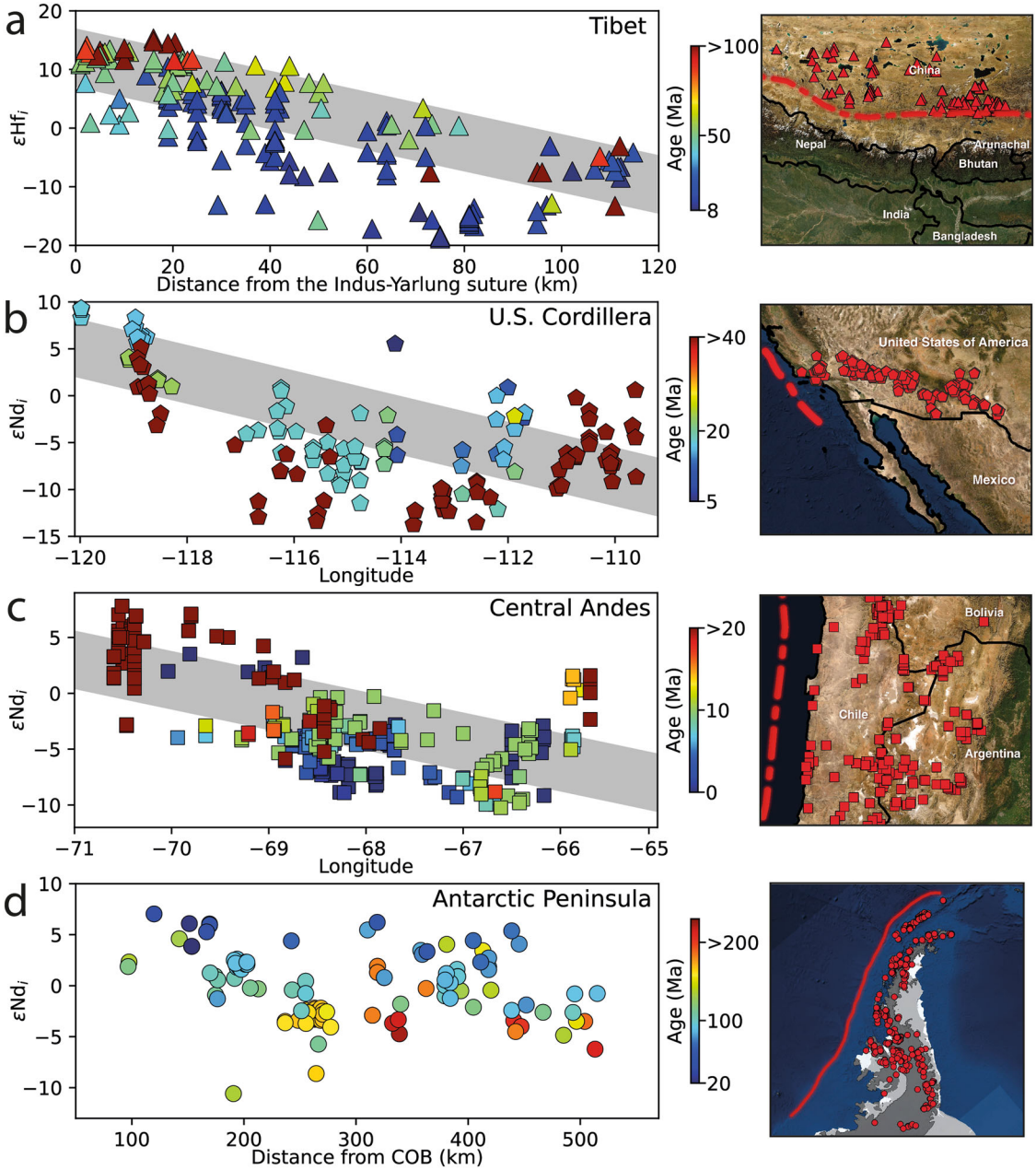

Fig. 6 | Comparison of the Antarctic Peninsula with other active margins. Compiled Hf and Nd isotopic data from igneous rocks for modern and ancient active margins in the left-hand panel. **a** Tibet, **b** U.S. Cordillera, **c** Central Andes, **d** Antarctic Peninsula. Magmatic isotopes are compared with their distance to the (palaeo-)trench and their crystallisation age (presented as a colour ramp). Sample locations are presented in the right-hand panels and were prepared with QGIS open-source software. Whilst Tibet, the U.S. Cordillera, and the Central Andes show a clear correlation between the distance to the trench and their isotopic composition, the Antarctic Peninsula active margin lacks such a clear relationship. Data from Tibet, U.S. Cordillera and Central Andes was obtained from ref. 2.

isotopically juvenile magmas. This migration occurred as a consequence of the progressively younger age of the subducted slab (Phoenix Plate) and the progressive decrease in convergence rate[22]. This led to the formation of melts that were derived by differing degrees of differentiation (i.e. from mafic to felsic compositions), but with a common and dominant isotopically juvenile signature. Furthermore, while these magmas differentiated to granitic compositions, they did not assimilate relevant amounts of old and isotopically evolved continental crust. Additionally, as older oceanic lithosphere is colder and as water is stored in the form of serpentine, fast subduction of old oceanic lithosphere allows the slab to remain hydrated until deeper in the mantle[52]; conversely, the slow subduction of young oceanic lithosphere has a reduced capacity to add volatiles to the lower crust. Therefore, as the rear of the arc migrated towards the trench during the Late Cretaceous–Cenozoic in the Antarctic Peninsula, the subducted slab had a lesser capacity to hydrate the continental plate above. This led to the establishment of narrow arc above a 'drier' lithospheric mantle beneath the Antarctic Peninsula lithosphere, which ultimately resulted in reduced capacity to incorporate older continental crustal material to these arc magmas. Additionally, the decrease in convergence rate that occurred throughout the Cenozoic would have reduced the friction between the subducting plate and the forearc[53,54]. Furthermore, the strength of the subduction interface critically controls the coupling between the subducted slab and the overriding plate[54]. This relative decoupling in the interface between the slab and the Antarctic Peninsula may also have played a role, in which the reduction of friction provided space that allowed young and juvenile asthenosphere to ascend to the lower continental crust. Therefore, as the arc

narrowed throughout the Late Cretaceous and Cenozoic, it incorporated magmas that were dominantly sourced from juvenile asthenospheric mantle and the arc magmas thus become progressively more juvenile with time.

The tectonic plate environment in which the Antarctic Peninsula developed is unique compared to other Cordilleran systems. The Tibetan active margin experienced the subduction of progressively older oceanic lithosphere[55] during the late Mesozoic and early Cenozoic, which transitioned into a continental collision[25]. The western U.S. Cordillera margin experienced a complex history with the subduction of the Farallon Plate[56,57] and the Juan de Fuca Plate, along with slab window processes[58] and the development of the large strike-slip San Andreas fault system[59]. The Central Andean margin underwent subduction of the Phoenix and Farallon plates[60], followed by the Nazca Plate after their consumption (which is currently subducting beneath South America[61]). Therefore, the Tibet, U.S. Cordillera and Central Andes active margins experienced a wide diversity of plate configurations and the subduction of different oceanic plates, which contrasts with the simpler subduction history of the Antarctic Peninsula. While isotopic trends can clearly provide information on the architecture and tectonic history of subduction as it has been clearly shown[2], the Antarctic Peninsula exhibits differing behaviour, and thus expands our understanding of how Cordilleran orogens evolve.

The role of arc magmatism in forming continental crust. The Hf isotopic compositions pre-Cretaceous zircons from the Antarctic Peninsula exhibit an evolution that mimics that of ancient, enriched lithospheric compositions[43] (Fig. 3a), whilst Cretaceous and younger zircons yield compositions suggesting the involvement of relatively more radiogenic sources. The pre-Cretaceous rocks that formed on the active margin of the Antarctic Peninsula were mainly derived from recycled Sunsas-aged crust (1.1-1.0 Ga[14,16,62]), and that juvenile continental crust mainly formed during the Cretaceous. The dataset presented here suggests that the formation of juvenile crust continued into the Cenozoic. Therefore, while the margin of the Antarctic Peninsula was active from the late Palaeozoic—early Mesozoic[14,18,30], it effectively generated juvenile crust from the Cretaceous onwards. This is contemporaneous with the progressively younger age of the subducting slab and its waning subduction rate, and therefore poses a link between the cessation of subduction and the effectiveness of a given active margin to generate juvenile crust. When considering the broader process of continental crustal growth and crustal recycling, this observation suggests that active margins undergoing waning subduction are more efficient at generating juvenile crust.

Methods

We combined new geochronological, geochemical and isotopic analyses on Cenozoic igneous rocks of the Antarctic Peninsula with a comprehensive collection of previous work on this region. This compilation is available in the Zenodo data repository (10.5281/zenodo.10605934). The whole rock geochemistry, whole rock (Nd-Sr) and mineral (Hf in zircon) isotopic tracing along with the zircon geochronology was acquired using the procedure presented in refs. 14–16,63–66. Additionally, we used the dataset presented in ref. 2 to compare our compilation of the Antarctic Peninsula with other active margins (i.e., Tibet, U.S. Cordillera and Central Andes).

Whole rock geochemistry

Agathe mill was used to prepare the whole rock powders, which were analysed using a Philips PW2400 X-Ray Fluorescence (XRF) spectrometer at the University of Lausanne, Switzerland. Standards NIMN, NIMG, BHVO and SY2 were used for quality control. Glass-fused disks were analysed for trace and rare earth elements (REE) by an Agilent 7700x quadrupole ICP-MS, which is also hosted at the University of Lausanne. NIST SRM 610 and 612 were used as external standards. The laser was set to a 10 Hz repetition rate and a spot size between 80 and 120 µm. While blanks were measured for ~90 s, standards and unknowns for 45 s. The Sr or Al_2O_3 concentrations obtained by XRF were used as an internal standard. Three ablations were performed by sample and their concentrations were calculated offline with LAMTRACE[67] and normalised to an anhydrous state in all diagrams. The uncertainties per sample are ±10% for REE and ±5% for other trace elements.

Sr-Nd whole rock isotopes

The powders prepared for the geochemical analyses were also used for the Sr-Nd whole rock isotopes, which were measured at the University of Geneva with a Thermo Neptune PLUS Multi-Collector ICP-MS following the procedure described by refs. 39,68. For this, it was required to dissolve 100 mg of whole rock powder in 4 ml of concentrated HF and 1 ml of 15 M HNO_3 in closed Teflon vials at 140 °C for 7 days. These solutions were dried down, to be after re-dissolved in 3 ml of 15 M HNO_3 and dried down again. Sr–Nd chemical separation followed the procedures described in refs. 69,70. While the internal fractionation was corrected using $^{88}Sr/^{86}Sr = 8.375209$ for the $^{87}Sr/^{86}Sr$ ratio and $^{146}Nd/^{144}Nd = 0.7219$ for the $^{143}Nd/^{144}Nd$ ratio; the external standards emplyed are SRM987 ($^{87}Sr/^{86}Sr = 0.710248$, long-term external reproducibility: 10 ppm) and JNdi-1 ($^{143}Nd/^{144}Nd = 0.512115$[71]; long-term external reproducibility: 10 ppm). Sr and Nd isotope ratios were further corrected for external fractionation by a value of −0.039 and +0.047 amu, respectively. ^{83}Kr and ^{85}Rb were monitored to correct the mass interferences at 84 (^{84}Kr), 86 (^{86}Kr) and 87 (^{87}Rb). Furthermore, ^{147}Sm was used ($^{144}Sm/^{147}Sm = 0.2067$) to correct the interference of ^{144}Sm on ^{144}Nd.

Zircon LA-ICP-MS U-Pb geochronology

Zircon U–Pb isotopic composition was collected at the University of Lausanne using an Element XR single-collector sector-field ICP-MS (Thermo Scientific). Ablations were performed with an UP-193FX ArF 193 nm excimer ablation system with a configuration that consisted in: 35 µm beam size, 5 Hz repetition rate, 30 s signal and 2.2–2.5 J/cm^2 of beam energy density. While the primary standard used was GJ-1 zircon (CA-ID-TIMS $^{206}Pb–^{238}U$ age of 600.5 ± 0.4 Ma[72,73]); the secondary standards were either Harvard 91500 (1065.4 ± 0.3 Ma[74]) zircon, or Plešovice (337.13 ± 0.37 Ma[75]) zircon. LAMTRACE[67] and IsoplotR[76] were used to calculate the dates, for which it was used only zircons yielding concordance greater than 90%.

Zircon in-situ Hf isotopes

The zircons used for U–Pb geochronology were also used for collecting in-situ Hf isotopes at the University of Geneva. These were obtained on a Thermo Neptune Plus MC-ICP-MS coupled to a Teledyne–Photon Machines Analyte G2 ArF excimer laser system equipped with a two-volume HelEx-2 ablation cell[77]. The configuration of the ablations consisted in a fluence of ~4 J/cm^2, a repetition rate of 5 Hz and a spot size of 40 µm or 50 µm. The carrier gas was He mixed with a small amount of N_2 before entering the Ar-plasma torch for sensitivity improvement. Low mass resolution was used to collect the measurements. Blanks and standards were analysed at the initiation, finalisation and every 15 analyses of unknown zircons. The standards used are Mud Tank, Plešovice, MUN4 and GJ-1 zircon.

Excel spreadsheets were used off-line to reduce the data, which consisted of the subtraction of (i) blanks and (ii) the isobaric interference of ^{176}Lu and ^{176}Yb on mass 176[78]. Additionally, the $^{176}Hf/^{177}Hf$ ratio was also corrected for mass bias[79]. βHf and βYb mass bias coefficients were calculated using the reference values of $^{179}Hf/^{177}Hf = 0.7325$[80] and $^{173}Yb/^{171}Yb = 1.1234$[81], respectively. Corrections for the isobaric interferences of ^{176}Yb and ^{176}Lu with ^{176}Hf were performed using $^{176}Yb/^{173}Yb = 0.786954$ and $^{176}Lu/^{175}Lu = 0.02645$, respectively[81]. The $^{206}Pb–^{238}U$ date of the respective crystal along with CHUR parameters ($^{176}Hf/^{177}Hf = 0.282785$[82], $^{176}Lu/^{177}Hf = 0.0336$[82] and $\lambda^{176}Lu = 1.87 \times 10^{-11}$ yr^{-1} [83]) were used to calculate $^{176}Hf/^{177}Hf_i$, and εHf_i.

Data availability

The detailed dataset necessary to inspect, interpret, replicate and build upon the methods reported in this article along with the source data used directly for generating the figures are available at the Zenodo repository:

10.5281/zenodo.10605934. This contains: (i) an exhaustive compilation of the geochronology, geochemistry and isotopic tracing data of the Antarctic Peninsula from previous work and (ii) all the files generated to report the new geochronological, geochemical and isotopic tracing data from northern Antarctic Peninsula herein presented.

Received: 12 July 2023; Accepted: 4 March 2024;
Published online: 27 March 2024

References

1. Ducea, M. N. & Barton, M. D. Igniting flare-up events in Cordilleran arcs. *Geology* **35**, 1047–1050 (2007).
2. Chapman, J. B., Ducea, M. N., Kapp, P., Gehrels, G. E. & DeCelles, P. G. Spatial and temporal radiogenic isotopic trends of magmatism in Cordilleran orogens. *Gondwana Res.* **48**, 189–204 (2017).
3. Bouilhol, P., Jagoutz, O., Hanchar, J. M. & Dudas, F. O. Dating the India–Eurasia collision through arc magmatic records. *Earth Planet. Sci. Lett.* **366**, 163–175 (2013).
4. Orozco-Esquivel, T., Petrone, M., Ferrari, C., Tagami, L. & Manetti, T. P. Geochemical and isotopic variability in lavas from the eastern Trans-Mexican Volcanic Belt: Slab detachment in a subduction zone with varying dip. *Lithos* **93**, 149–174 (2007).
5. Regelous, M., Collerson, K. D., Ewart, A. & Wendt, J. I. Trace element transport rates in subduction zones: evidence from Th, Sr and Pb isotope data for Tonga-Kermadec arc lavas. *Earth Planet. Sci. Lett.* **150**, 291–302 (1997).
6. Kay, S. M., Godoy, E. & Kurtz, A. Episodic arc migration, crustal thickening, subduction erosion, and magmatism in the south-central Andes. *GSA Bull.* **117**, 67–88 (2005).
7. Kay, S. M., Coira, B. & Viramonte, J. Young mafic back arc volcanic rocks as indicators of continental lithospheric delamination beneath the Argentine Puna Plateau, central Andes. *J. Geophys. Res. Solid Earth* **99**, 24323–24339 (1994).
8. Haschke, M., Siebel, W., Günther, A. & Scheuber, E. Repeated crustal thickening and recycling during the Andean orogeny in north Chile (21°–26°S). *J. Geophys. Res. Solid Earth* **107**, 6–18 (2002). ECV 6-1-ECV.
9. DePaolo, D. J. & Daley, E. E. Neodymium isotopes in basalts of the southwest basin and range and lithospheric thinning during continental extension. *Chem. Geol.* **169**, 157–185 (2000).
10. Kay, R. W. & Kay, S. M. Crustal recycling and the Aleutian arc. *Geochim. Cosmochim. Acta* **52**, 1351–1359 (1988).
11. Leat, P. T., Scarrow, J. H. & Millar, I. L. On the Antarctic Peninsula batholith. *Geol. Mag.* **132**, 399–412 (1995).
12. Robert Wallace. *The San Andreas Fault System, California*. *Professional Paper.* https://pubs.usgs.gov/publication/pp1515, https://doi.org/10.3133/pp1515 (1990).
13. Bastias, J. et al. The Byers Basin: Jurassic-Cretaceous tectonic and depositional evolution of the forearc deposits of the South Shetland Islands and its implications for the northern Antarctic Peninsula. *Int. Geol. Rev.* **62**, 1467–1484 (2019).
14. Bastias, J. et al. The Gondwanan margin in West Antarctica: insights from Late Triassic magmatism of the Antarctic Peninsula. *Gondwana Res.* **81**, 1–20 (2020).
15. Bastias, J. et al. A revised interpretation of the Chon Aike magmatic province: active margin origin and implications for the opening of the Weddell Sea. *Lithos* **386–387**, 106013 (2021).
16. Bastias, J. et al. Cretaceous magmatism in the Antarctic Peninsula and its tectonic implications. *J. Geol. Soc.* **180**, jgs2022-067 (2022).
17. Riley, T. R., Flowerdew, M. J., Millar, I. L. & Whitehouse, M. J. Triassic magmatism and metamorphism in the Antarctic Peninsula: identifying the extent and timing of the Peninsula. *Orogeny. J. South Am. Earth Sci.* **103**, 102732 (2020).
18. Riley, T. R. et al. Palaeozoic—Early Mesozoic geological history of the Antarctic Peninsula and correlations with Patagonia: kinematic reconstructions of the proto-Pacific margin of Gondwana. *Earth-Sci. Rev.* **236**, 104265 (2023).
19. Gao, L. et al. New paleomagnetic constraints on the cretaceous tectonic framework of the Antarctic Peninsula. *J. Geophys. Res. Solid Earth* **126**, e2021JB022503 (2021).
20. Gao, L. et al. Plate rotation of the Northern Antarctic Peninsula since the Late Cretaceous: implications for the tectonic evolution of the Scotia Sea region. *J. Geophys. Res. Solid Earth* **128**, e2022JB026110 (2023).
21. Twinn, G., Riley, T., Fox, M. & Carter, A. Thermal history of the southern Antarctic Peninsula during Cenozoic oblique subduction. *J. Geol. Soc.* **179**, jgs2022–008 (2022).
22. Burton-Johnson, A., Bastias, J. & Kraus, S. Breaking the ring of fire: how ridge collision, slab age, and convergence rate narrowed and terminated the Antarctic continental arc. *Tectonics* **42**, e2022TC007634 (2023).
23. Boekhout, F., Roberts, N. M. W., Gerdes, A. & Schaltegger, U. A Hf-isotope perspective on continent formation in the south Peruvian Andes. *Geol. Soc. Lond. Spec. Publ.* **389**, 305–321 (2015).
24. Oliveros, V. et al. Lithospheric evolution of the pre- and early Andean convergent margin, Chile. *Gondwana Res.* **80**, 202–227 (2020).
25. Yin, A. & Harrison, T. M. Geologic evolution of the Himalayan-Tibetan Orogen. *Annu. Rev. Earth Planet. Sci.* **28**, 211–280 (2000).
26. Spikings, R., & Van der Lelij, R. The geochemical and isotopic record of Wilson cycles in Northwestern South America: from the Iapetus to the Caribbean. *Geosciences* **12**, 5 (2022).
27. Hole, M. J., Pankhurst, R. & Saunders, A. D. Geochemical evolution of the Antarctic Peninsula magmatic arc; the importance of mantle-crust interactions during granitoid genesis. *The Geological Evolution of Antarctica* 369–374 (Cambridge University Press, 1991).
28. Millar, I. L., Willan, R. C. R., Wareham, C. D. & Boyce, A. J. The role of crustal and mantle sources in the genesis of granitoids of the Antarctic Peninsula and adjacent crustal blocks. *J. Geol. Soc.* **158**, 855–867 (2001).
29. Burton-Johnson, A. & Riley, T. R. Autochthonous v. accreted terrane development of continental margins: a revised in situ tectonic history of the Antarctic Peninsula. *J. Geol. Soc.* **172**, 822–835 (2015).
30. Castillo, P., Fanning, C. M. & Riley, T. R. Zircon O and Hf isotopic constraints on the genesis of Permian–Triassic magmatic and metamorphic rocks in the Antarctic Peninsula and correlations with Patagonia. *J. South Am. Earth Sci.* **104**, 102848 (2020).
31. Birkenmajer, K., Andrzej, G., Kreuzer, H. & Muller, P. K-Ar dating of the Melville Glaciation (Early Miocene) in West Antarctica. *Bull. Pol. Acad. Sci. Earth Sci.* **33**, 1523 (1985).
32. Larter, R. & Barker, P. Effects of ridge crest-trench interaction on Antarctic-Phoenix Spreading: forces on a young subducting plate. *J. Geophys. Res. Solid Earth* **96**, 19583–19607 (1991).
33. Jin, Y. K., Lee, J., Hong, J. K. & Nam, S. H. Is subduction ongoing in the South Shetland Trench, Antarctic Peninsula? New constraints from crustal structures of outer trench wall. *Geosci. J.* **13**, 59–67 (2009).
34. González-Casado, J. M., Robles, J. L. G. & López-Martínez, J. Bransfield Basin, Antarctic Peninsula: not a normal Backarc basin. *Geology* **28**, 1043–1046 (2000).
35. Fretzdorff, S. et al. Magmatism in the Bransfield Basin: rifting of the South Shetland arc? *J. Geophys. Res. Solid Earth* **109**, B12208, 1–19, (2004).
36. Smellie, J. L. Geochemistry and tectonic setting of alkaline volcanic rocks in the Antarctic Peninsula: a review. *J. Volcanol. Geotherm. Res.* **32**, 269–285 (1987).
37. Košler, J. et al. Combined Sr, Nd, Pb and Li isotope geochemistry of alkaline lavas from northern James Ross Island (Antarctic Peninsula) and implications for back-arc magma formation. *Chem. Geol.* **258**, 207–218 (2009).
38. Zheng, Y.-F. Subduction zone geochemistry. *Geosci. Front.* **10**, 1223–1254 (2019).

39. Chiaradia, M. Crustal thickness control on Sr/Y signatures of recent arc magmas: an Earth scale perspective. *Sci. Rep.* **5**, 8115 (2015).
40. Chapman, J. B., Ducea, M. N., DeCelles, P. G. & Profeta, L. Tracking changes in crustal thickness during orogenic evolution with Sr/Y: an example from the North American Cordillera. *Geology* **43**, 919–922 (2015).
41. Ducea, M. N., Saleeby, J. B. & Bergantz, G. The architecture, chemistry, and evolution of continental magmatic arcs. *Annu. Rev. Earth Planet. Sci.* **43**, 299–331 (2015).
42. Oliveros, V. et al. The early stages of the magmatic arc in the Southern Central Andes. *The Evolution of the Chilean-Argentinean Andes* (eds. Folguera, A. et al.) 165–190 (Springer International Publishing, Cham, 2018). https://doi.org/10.1007/978-3-319-67774-3_7.
43. Griffin, W. L. et al. Zircon chemistry and magma mixing, SE China: in-situ analysis of Hf isotopes, Tonglu and Pingtan igneous complexes. *Lithos* **61**, 237–269 (2002).
44. Barker, P. F. The Cenozoic subduction history of the Pacific margin of the Antarctic Peninsula: ridge crest–trench interactions. *J. Geol. Soc.* **139**, 787–801 (1982).
45. Jordan, T. A. et al. Structure and evolution of Cenozoic arc magmatism on the Antarctic Peninsula: a high-resolution aeromagnetic perspective. *Geophys. J. Int.* **198**, 1758–1774 (2014).
46. Livermore, R. et al. Autopsy on a dead spreading center: the Phoenix Ridge, Drake Passage, Antarctica. *Geology* **28**, 607–610 (2000).
47. Farmer, G. L. & DePaolo, D. J. Origin of Mesozoic and tertiary granite in the Western United States and implications for Pre-Mesozoic crustal structure: 1. Nd and Sr isotopic studies in the geocline of the Northern Great Basin. *J. Geophys. Res. Solid Earth* **88**, 3379–3401 (1983).
48. Pankhurst, R. J., Hole, M. J. & Brook, M. Isotope evidence for the origin of Andean granites. *Earth Environ. Sci. Trans. R. Soc.* **79**, 123–133 (1988).
49. Faure, G. & Mensing, T. Isotopes: Principles and Applications, 3rd Edition (Wiley, 2005).
50. Faure, G. Origin of Igneous Rocks: The Isotopic Evidence (Springer, Berlin, 2001).
51. Guenthner, W. R., Barbeau Jr., D. L., Reiners, P. W. & Thomson, S. N. Slab window migration and terrane accretion preserved by low-temperature thermochronology of a magmatic arc, Northern Antarctic Peninsula. *Geochem. Geophys. Geosyst.* **11**, 1–13 (2010).
52. Magni, V., Bouilhol, P. & van Hunen, J. Deep water recycling through time. *Geochem. Geophys. Geosyst.* **15**, 4203–4216 (2014).
53. Meade, B. J. & Conrad, C. P. Andean growth and the deceleration of South American subduction: time evolution of a coupled orogen-subduction system. *Earth Planet. Sci. Lett.* **275**, 93–101 (2008).
54. Tan, E., Lavier, L. L., Van Avendonk, H. J. A. & Heuret, A. The role of frictional strength on plate coupling at the subduction interface. *Geochem. Geophys. Geosyst.* **13**, 1–19 (2012).
55. Vérard, C., Stampfli, G., Borel, G. & Hochard, C. The Indian promontory: a bridge between plate tectonics and life evolution models. *Univ. J. Geosci.* **5**, 25–32 (2017).
56. Liu, L., Spasojević, S. & Gurnis, M. Reconstructing Farallon plate subduction beneath North America back to the late cretaceous. *Science* **322**, 934–938 (2008).
57. Liu, S. & Currie, C. A. Farallon plate dynamics prior to the Laramide orogeny: numerical models of flat subduction. *Tectonophysics* **666**, 33–47 (2016).
58. McCrory, P. A., Wilson, D. S. & Stanley, R. G. Continuing evolution of the Pacific–Juan de Fuca–North America slab window system—a trench–ridge–transform example from the Pacific Rim. *Tectonophysics* **464**, 30–42 (2009).
59. Powell, R. E. & Weldon, R. J. Evolution of the San Andreas fault. *Annu. Rev. Earth Planet. Sci.* **20**, 431–468 (1992).
60. Somoza, R. & Ghidella, M. E. Late Cretaceous to recent plate motions in western South America revisited. *Earth Planet. Sci. Lett.* **331–332**, 152–163 (2012).
61. Giambiagi, L. et al. Crustal anatomy and evolution of a subduction-related orogenic system: insights from the Southern Central Andes (22-35°S). *Earth Sci. Rev.* **232**, 104138 (2022).
62. Goodge, J. W. & Fanning, C. M. Mesoarchean and Paleoproterozoic history of the Nimrod complex, central Transantarctic mountains, Antarctica: stratigraphic revisions and relation to the Mawson Continent in East Gondwana. *Precambrian Res.* **285**, 242–271 (2016).
63. Bastias, J. et al. Data on the arc magmatism developed in the Antarctic Peninsula and Patagonia during the Late Triassic–Jurassic: a compilation of new and previous geochronology, geochemistry and isotopic tracing results. *Data Brief* **36**, 107042 (2021).
64. Cochrane, R. et al. Permo-Triassic anatexis, continental rifting and the disassembly of western Pangaea. *Lithos* **190–191**, 383–402 (2014).
65. Cochrane, R. et al. Distinguishing between in-situ and accretionary growth of continents along active margins. *Lithos* **202–203**, 382–394 (2014).
66. van der Lelij, R., Spikings, R., Ulianov, A., Chiaradia, M. & Mora, A. Palaeozoic to Early Jurassic history of the northwestern corner of Gondwana, and implications for the evolution of the Iapetus, Rheic and Pacific Oceans. *Gondwana Res.* **31**, 271–294 (2016).
67. Jackson, S. LAMTRACE data reduction software for LA-ICP-MS.*Laser Ablation ICP-MS Earth Sci. Curr. Pract. Outst. Issues* **40**, 305–307 (2008).
68. Béguelin, P., Chiaradia, M., Beate, B. & Spikings, R. The Yanaurcu volcano (Western Cordillera, Ecuador): a field, petrographic, geochemical, isotopic and geochronological study. *Lithos* **218–219**, 37–53 (2015).
69. Pin, C. & Zalduegui, J. S. Sequential separation of light rare-earth elements, thorium and uranium by miniaturized extraction chromatography: application to isotopic analyses of silicate rocks. *Anal. Chim. Acta* **339**, 79–89 (1997).
70. Chiaradia, M., Müntener, O. & Beate, B. Enriched basaltic andesites from mid-crustal fractional crystallization, recharge, and assimilation (Pilavo Volcano, Western Cordillera of Ecuador). *J. Petrol.* **52**, 1107–1141 (2011).
71. Tanaka, T. et al. JNdi-1: a neodymium isotopic reference in consistency with LaJolla neodymium. *Chem. Geol.* **168**, 279–281 (2000).
72. Boekhout, F. et al. Mesozoic arc magmatism along the southern Peruvian margin during Gondwana breakup and dispersal. *Lithos* **146–147**, 48–64 (2012).
73. Ulianov, A., Müntener, O., Schaltegger, U. & Bussy, F. The data treatment-dependent variability of U–Pb zircon ages obtained using mono-collector, sector field, laser ablation ICPMS. *J. Anal. At. Spectrom.* **27**, 663–676 (2012).
74. Wiedenbeck, M. et al. Three natural zircon standards for U-Th-Pb, Lu-Hf, trace element and ree analyses. *Geostand. Newsl.* **19**, 1–23 (1995).
75. Sláma, J. et al. Plešovice zircon—a new natural reference material for U–Pb and Hf isotopic microanalysis. *Chem. Geol.* **249**, 1–35 (2008).
76. Vermeesch, P. IsoplotR: a free and open toolbox for geochronology. *Geosci. Front.* **9**, 1479–1493 (2018).
77. d'Abzac, F.-X., Czaja, A. D., Beard, B. L., Schauer, J. J. & Johnson, C. M. Iron distribution in size-resolved aerosols generated by UV-femtosecond laser ablation: influence of cell geometry and implications for in situ isotopic determination by LA-MC-ICP-MS. *Geostand. Geoanal. Res.* **38**, 293–309 (2014).
78. Fisher, C. M. et al. Synthetic zircon doped with hafnium and rare earth elements: a reference material for in situ hafnium isotope analysis. *Chem. Geol.* **286**, 32–47 (2011).
79. Albarède, F. et al. Precise and accurate isotopic measurements using multiple-collector ICPMS1. *Geochim. Cosmochim. Acta* **68**, 2725–2744 (2004).
80. Patchett, P. J. & Tatsumoto, M. A routine high-precision method for Lu-Hf isotope geochemistry and chronology. *Contrib. Miner. Petrol.* **75**, 263–267 (1981).

81. Thirlwall, M. F. & Anczkiewicz, R. Multidynamic isotope ratio analysis using MC–ICP–MS and the causes of secular drift in Hf, Nd and Pb isotope ratios. *Int. J. Mass Spectrom.* **235**, 59–81 (2004).
82. Bouvier, A., Vervoort, J. D. & Patchett, P. J. The Lu–Hf and Sm–Nd isotopic composition of CHUR: Constraints from unequilibrated chondrites and implications for the bulk composition of terrestrial planets. *Earth Planet. Sci. Lett.* **273**, 48–57 (2008).
83. Söderlund, U., Patchett, P. J., Vervoort, J. D. & Isachsen, C. E. The 176Lu decay constant determined by Lu–Hf and U–Pb isotope systematics of Precambrian mafic intrusions. *Earth Planet. Sci. Lett.* **219**, 311–324 (2004).
84. Larter, R. D., Rebesco, M., Vanneste, L. E., GambôA, L. A. P. & Barker, P. F. Cenozoic tectonic, sedimentary and glacial history of the Continental Shelf west Of Graham Land, Antarctic Peninsula. in (eds. Barker, P. F. & Cooper, A. K.) 1–27 (American Geophysical Union, Washington, D.C., 1997).
85. Maniar, P. D. & Piccoli, P. M. Tectonic discrimination of granitoids. *Geol. Soc. Am. Bull.* **101**, 635–643 (1989).
86. Zen, E. Phase relations of peraluminous granitic rocks and their petrogenetic implications. *Annu. Rev. Earth Planet. Sci.* **16**, 21–51 (1988).
87. Pearce, J., Harris, N. & Tindle, A. Trace element discrimination diagrams for the tectonic interpretation of granitic rocks. *J. Petrol.* **25**, 956–983 (1984).
88. Sun, S. S., & McDonough, W. F. Chemical and isotopic systematics of oceanic basalts: implications for mantle composition and processes. *Geol. Soc. Lond. Spec. Publ* **42**, 313–345 (1989).

Acknowledgements

J.B. was funded by the Swiss National Science Foundation (project P5R5PN_217947) and the project RT-01-22 was funded by the Chilean Antarctic Institute (INACH). Fieldwork on the Antarctic Peninsula was supported by the Chilean Antarctic Institute. The authors thanks for the loan of rocks by the British Antarctic Survey and the Polar Rock Repository at Ohio State University. Authors thanks Alexey Ulianov for his assistance on the LA-ICP-MS at the University of Lausanne and to César Ordoñez from the University of Geneva for his support developing the figures. JB thanks Richard Spikings for his support and guidance throughout his doctorate. DC acknowledges support from Science Foundation Ireland (SFI) under Grant Number 13/RC/2092 and 13/RC/2092_P2 (SFI Research Centre in Applied Geosciences, iCRAG). New data presented herein is based on (i) field sampling campaigns funded by INACH and (ii) samples provided by the British Antarctic Survey and the Polar Rock Repository with support from the National Science Foundation, under Cooperative Agreement OPP-1643713.

Author contributions

Joaquin Bastias-Silva: Conceptualisation, methodology, data curation, formal analysis, writing—original draft, writing—review and editing. Alex Burton-Johnson: Formal analysis, writing—original draft, writing—review and editing. David Chew: Writing—original draft, writing—review and editing. Teal Riley: Data curation, writing—original draft, writing—review and editing. Wuidad Jara: Formal analysis. Massimo Chiaradia: Data curation.

Competing interests

The authors declare no competing interests.

Additional information

Supplementary information The online version contains supplementary material available at https://doi.org/10.1038/s43247-024-01301-1.

Correspondence and requests for materials should be addressed to Joaquin Bastias-Silva.

Peer review information *Communications Earth & Environment* thanks Malcolm Hole and David Barbeau for their contribution to the peer review of this work. Primary Handling Editor: Joe Aslin. A peer review file is available.